P2.138 ENSEMBLE KALMAN FILTER ASSIMILATION OF COASTAL WSR88D RADAR DATA AND FORECASTING FOR HURRICANE IKE (2008)

Jili Dong * and Ming Xue
Center for Analysis and Prediction of Storms and School of Meteorology
University of Oklahoma, Norman, Oklahoma 73072

1. Introduction

Landfalling hurricanes can pose deadly threats to many lives and cause loss of billions of dollars. Numerical prediction of the hurricane track has improved greatly in recent years but the improvement to hurricane intensity forecasting has been limited (Houze et al. 2007). Radar is one of the most effective observation platforms to provide essential information on hurricane structure at high temporal and spatial resolutions. When assimilated into high-resolution numerical models, radar observations can help to create more accurate initial conditions and lead to improved the intensity forecasts (e.g., Zhang et al. 2009; Zhao and Xue 2009).

Among advanced data assimilation methods, the ensemble Kalman filter (EnKF) employs ensemble forecasts to estimate flow-dependent background error covariance. Its simple formulation and easy implementation compared to four-dimensional variational data assimilation method, allow it to enjoy popularity within the research community. It was first proposed by Evensen (1994) and has bred an array of variants since then. As one of these variants, the serial ensemble square root filter (Whitaker and Hamill 2002, EnSRF) is chosen to assimilate radar observations in this study.

The specific case in this study, Hurricane Ike (2008), started as a tropical disturbance near Cape Verde and developed into a category 4 hurricane during its strongest stage. It made landfall in Galveston, Texas at 07:00 UTC 13 September as a category 2 hurricane. Before and after Ike's landfall in the U.S., it caused 32 billion dollars of damage and 112 deaths in the U.S., making it the third costliest hurricane in U.S. history. This study investigates the effect of assimilating radar reflectivity and radial velocity data from coastal WSR-88D radars using EnKF on the analysis and forecast of Ike.

* *Corresponding author address:* Jili Dong, Univ. of Oklahoma, School of Meteorology, Norman, OK, 73072; email: jldong@ou.edu.

2. Prediction Model and EnKF Configurations

The Advanced Regional Prediction System (ARPS, Xue et al. 2004) is used in this study as the prediction model. A 515x515x53 grid with a horizontal resolution of 4 km defines the whole physical domain. Mean vertical grid spacing is 625 m with a vertical grid stretching scheme having a grid spacing of 50 m at the surface. The Lin microphysical scheme is used along with the 1.5 TKE-based sub-grid scale turbulence and PBL parameterizations. Details on these physics options can be found in Xue et al. (2001; 2003) Coastal WSR-88D radars at Houston-Gavelston, Texas (KHGX) and Lake Charles, Louisiana (KLCH) provide the coverage for Ike when it approached to the east Texas coast. Reflectivity (Z) and radial velocity (Vr) data from these two radars are assimilated with observation errors specified as 2 dBZ and 1 ms^{-1}, respectively. The Vr from Level-II data is further manually quality-controlled with the NCAR SOLO software to ensure correct velocity dealising.

The baseline control forecast without radar data assimilation (NoDA) is run from 0600 UTC 13 September, initialized with NCEP GFS analysis. In all other experiments with radar data assimilation, Gaussian random perturbations smoothed to have 100 km horizontal correlation scales are added in the whole domain to initialize the 32-member ensemble at 2200 UTC 12 September. Six-hour-long ensemble forecasts were made from these perturbed initial conditions to allow evolved background error covariance to develop. At 0400 UTC 13 September, another set of perturbations with a smaller horizontal de-correlation scale of 12 km is added to the forecast fields in the observed precipitation regions only to introduce storm-scale perturbations.

The first set of experiments in which 10-minute-long assimilation cycles are employed, Vr alone, Z alone and both Vr and Z are assimilated, respectively, in expereiments named ExpVr, ExpZ and ExpAll. In these experiments, The first EnKF analysis of radar data occurs at 0410 UTC, and the assimilation cycles end at 0600 UTC 13 September. Two additional experiments, named Exp30Min and Exp60Min, are performed which has the same assimilation window length but only assimilate Vr and Z data every 30 and 60 minutes, respectively. At the end of the assimilation window, at 0600 UTC, 18-hour-long deterministic forecast and an ensemble of forecasts are performed until 0000 UTC 14 September. To reduce sampling error caused by the small ensemble, a prior multiplicative covariance inflation of 5% and posterior additive error are used. A covariance localization to limit the spatial impact of the observations has cutoff radii of 12 km in the horizontal and 4 km in the vertical. The inflation and location parameters were chosen based on a number of sensitivity experiments.

3. Spread, innovation and increment

The EnKF relies on a sufficiently accurate estimate of the background error covariance to update the state variables. Due to sampling error and the lack of explicit representation of model, the forecast ensemble tend to be underdispersive. Maintaining adequate ensemble spread is necessary to prevent filter divergence. An examination of the spread of the state variables in the precipitation region during the analysis cycles of ExpAll (Fig. 1) reveals that for the horizontal wind components and pressure, the largest spread reduction by the EnKF analysis occurs in the first two cycles, suggesting more observation impact during those cycles. Despite the gradual reduction in the forecast spread in the subsequent cycles, the variances of the state variables remain at a reasonable level, which was helped by multiplicative and additive inflation.

The observation innovations, or the rms difference between observations and the state projected to the observations, denoted as y-H(x), measure how well the model state fit the observations. The root-mean-square (rms hereafter) innovations of ExpAll averaged in precipitation region are shown in Fig. 2 for the background forecasts and analyses. With respect to both radars, the rms innovations of both Z and Vr have the largest reduction in the first two assimilation cycles. After 10 to 20 minutes of forecast and analysis, the innovation reductions remain and continue until the end of the analysis cycles. At the end, the rms innovations of Vr and Z are 2 to 4 ms^{-1} and 5 dBZ, respectively, which are much smaller than the initial values of about 10 ms^{-1} and 20 dBZ, respectively. This says that both the forecast and analysis states are significantly improved, in terms of the fit to observations, by the EnKF data assimilation.

To better understand the behavior of radar data analysis, the increments of horizontal wind components in the first and last analysis cycles are plotted in Fig. 3. It is found that during the first analysis at 0410 UTC, the horizontal wind increments appear to systematically enhance the hurricane vortex, with the increment having a well-organized structure of cyclonic rotation (Fig. 3a). At the end of the analysis cycles, the wind increments are much less organized, indicating that most of the corrections now corresponding to storm-scale structures at the sub-vortex scale (Fig. 3b). The error in the overall vortex of the background forecast has been significantly reduced by this time.

4. Impact on the analysis and deterministic forecast

4.1 Impact on structure

The composite reflectivity and horizontal wind vectors at the 3 km height from NoDA, ExpVr, ExpZ and ExpAll are presented in Fig. 4, together with the observed composite reflectivity (OBS). The stronger and tighter inner cores in the final analyses are identified with all radar data assimilation experiments, compared that in the GFS analysis at 0600 UTC. The reflectivity field in ExpVr shows a broader and stronger rainband than observations (Fig. 4c). There is no reflectivity in the GFS analysis. ExpAll and ExpZ have similar rainband structures and are closer to the observations than ExpVr (Fig. 4d-e). This difference is also reflected in rms innovations of Z at this time (not shown), where for both radars, Z rms innovation is about 15 dBZ in ExpVr and only about 5 dBZ in ExpAll and ExpZ.

In the 6-hour forecast, the center of Ike is over the land north of Houston. Generally, all experiments with radar data assimilation display a more tightly wrapped rainband than NoDA. NoDA also has a spiral rainband on the north-west of the vortex center, which is too strong compared with the observation (Fig. 4f-j).

During 6 additional hours of forecast, the rainband in Ike moves further inland and an axis-asymmetric structure is seen on Fig. 4k. Two major precipitation regions covering eastern Texas developed in the north-west and south-east quadrants around the vortex center. A clear-air hole without precipitation is visible in the vortex center in NoDA (Fig. 4l). With the radar data assimilated, the clear-air hole diminishes or disappears, and the precipitation patterns are closer to the observations (Fig. 4m-o). Amid the radar data assimilation experiments, ExpZ has a broader precipitation region in the south-east part and a tighter inner core, more similar to the observations (Fig. 4n).

At the final forecast time of 0000 UTC 14 September, most of the precipitation is out of Texas. The interaction with the cold front system to the north and the moisture transport from the Gulf lead to rainfall in Oklahoma and Arkansas and a more axis-asymmetric structure (Fig. 4p). The clear-air hole in the vortex center is still identifiable in NoDA (Fig. 4q). The rainbands in experiments with radar data are still more tightly wrapped. Like the observations, the hurricane eyes in ExpZ and ExpAll are filled with precipitation, and precipitation patterns in these two experiments are the closest to the observations (Fig. 4s and t).

4.2 Intensity and track

The minimum sea level pressure (MSLP) every 3 hours during the 18 hours of forecast from all experiments are plotted in Fig. 5b, along with the best track MSLP from the National Hurricane Center. All experiments with radar data exhibit solid improvement over NoDA during the first 12 hours for intensity forecast. The analyzed MSLPs of 955 mb in ExpVr and ExpAll at 0600 UTC are significantly lower than the 975 mb of NoDA, although still somewhat higher than the best track value of 951 mb. Assimilation of Z alone leads to a mild improvement of 9 mb over NoDA at 0600 UTC, resulting in a weaker vortex than assimilating Vr or Vr plus Z. The intensity of NoDA is too weak and does not change dramatically during the first 12 hours of forecast while the best track hurricane keeps weakening until 2100 UTC. ExpVr and ExpAll both capture the pressure rise at similar rate as the best track data before 1500 UTC. Between 1500 to 2100 UTC, the best track data show faster weakening than earlier, which is not reflected in any of the radar data assimilation experiments. The prediction model error could have contributed to this discrepancy, in addition to possible initial condition error.

The predicted tracks from all experiments are plotted in Fig. 5a, along with the best track. Even with a quite accurate initial position of only 7 km track error in the GFS analysis at 0600 UTC 13 September, NoDA takes a west-most path in the 18-hour forecast. The track error increases with the forecast time and reaches 80 km at 0000 UTC 14 September (Fig. 5c). With radar data assimilation, the track errors at 0600 UTC are all larger than NoDA. One problem related to the larger track error at the initial time is identified. The initial track of the deterministic forecast is determined by finding the MSLP center in the mean field of the 32 member ensemble. After averaging the members, the mean field exhibits an elongated vortex owing to the hurricane position spread in the ensemble members. This creates some uncertainty with the vortex center estimation. An average of the tracks among all individual members provides a better result with an initial track error reduction of 10 km for ExpAll (Fig. 9a and c). All predicted tracks in the data assimilation experiments are closer to the best track than in NoDA, with the mean track errors in all being less than 20 km. Although ExpZ has a larger mean track error of 18 km compared to ExpVr and ExpAll, it is encouraging to see that assimilating Z alone still results in 56% improvement in track forecasting on average over NoDA.

4.3 Precipitation

Flooding caused by Ike was one of the major culprits of deaths and economy loss, highlighting the importance of precipitation forecast. Fig. 6 shows the 18-hour accumulated precipitation for all experiments along with the Stage IV precipitation data. The observations show that the maximum accumulated rainfall is positioned around Huntsville and Conroe, Texas, north of Houston (Fig. 6a). NoDA fails to predict this strong rainfall region completely (Fig. 6b). Assimilation of radar data helps to capture this intense precipitation area in the three data assimilation experiments although the strength and area coverage are under-predicted (Fig. 6c-e). For the lighter or stratiform precipitation, it is not easy to tell which experiment has a better prediction.

To quantify the precipitation forecast skills, equitable threat scores (ETS hereafter) for 3-

hourly accumulated precipitation are calculated and plotted for all experiments in Fig. 7. A threshold of 30 mm is chosen to present convective rainfall. In the first 6 hours of forecast, all experiments with radar data have higher ETS scores than NoDA. From 1200 UTC to 1800 UTC, the score is still higher in ExpZ while those of ExpAll and ExpVr are close to that of NoDA. There are increases in ETS scores for ExpAll and ExpVr from 1800 to 2100 UTC, which needs further examination. At the end of forecast, all experiments have their scores below 0.1, partly due to the shrunken area of convective precipitation at this time; in this situation, small position errors could lead to very low scores.

The ETS of 18-hour accumulated precipitation is also calculated (Fig. 8) for four thresholds ranging from 30 mm to 120 mm. It is noted that for all the thresholds, radar data assimilation helps to improve the quantative precipitation forecast. The larger the threshold is, the stronger the relative improvement is, implying more importance in improving convective precipitation forecast. For the 120 mm threshold, the relative improvements of three radar data assimilation experiments over NoDA are around 300%.

5. Ensemble forecast

The EnKF provides an ensemble of analyses which can be used to initialize an ensemble of forecasts. Thirty two ensemble forecasts are therefore carried out from the 0600 UTC analyses of ExpAll. The intensities, tracks and ETS scores of the ensemble forecasts are plotted in Fig. 9. The results of the deterministic forecast starting from the ensemble mean analysis and the mean of ensemble forecasts are also shown for comparison. Because Ike is in a weakening stage during this forecast period, the spread of the ensemble forecasts in intensity did not increase noticeably with time (Fig. 9b). It is also found in other studies that the intensity error growth of a decaying hurricane system is not as strong as an intensifying one and the ensemble spread tends to decrease with time (see Fig. 12. of Zhang et al. 2009). The mean of ensemble MSLPs is similar with that of the deterministic forecast.

An increase in uncertainty is observed in the ensemble track forecasts (Fig. 9a). The variance of the center position is increased at the end of forecast. This trend is also reflected in the predicted track error. It should be noted that the calculation of track error spread could conceal the actual large track spread among the members where two widely separated vortex center could have similar track errors. As mentioned before, the average position of ensemble members is closer to the best track than the single ensemble mean at 0600 UTC. The predicted track of the ensemble average also has certain improvement over the deterministic forecast at 1500 and 1800 UTC (Fig. 9c), suggesting the potential benefit of using ensemble mean for hurricane track prediction.

ETS scores are also calculated for the ensemble forecasts (Fig. 10). At most forecast times, most of the ensemble members have higher scores than NoDA. Similar to track error, we should be very cautious when using ETS scores to estimate the precipitation forecast uncertainty as two highly different precipitation forecasts can have very similar ETS scores.

6. Sensitivity of assimilation interval

The data assimilation interval is changed to test the assimilation frequency’s impact on intensity, track and precipitation forecast (Fig. 11). The intensity forecasts indicate the 60-minute interval is not enough to predict a vortex as strong as 10-minure and 30-minute in terms of MSLP (Fig. 11b). The latter two have similar intensity forecasts while MSLP in 10-minute interval is closer to the best track during the first 3 hour forecast. All the three intervals show similar track forecasts while 30-minute interval has the smallest mean track error (Fig. 11a and c). The ETS scores show all of the three intervals share the close precipitation forecast (not shown).

7. Summary

The impact of radar data assimilation with EnKF on the analysis and forecast of Hurricane Ike’s intensity, track and precipitation is investigated in this study. Radial velocity and reflectivity bservations from two coastal radars are assimilated within a 2 hour long window. With the prior multiplicative and posterior additive inflations, the ensemble spread is well maintained and large impacts from the observations are obtained on the analyzed wind and microphysical fields.

The assimilation of radar observations is found to significantly improve the structure, intensity, track and precipitation forecasts of Ike. Assimilating Vr alone leads to a much larger improvement to the intensity forecast than Z alone. For track forecast, Vr alone produces a slightly better forecast than Z alone. Z alone results in an precipitation forecast improvement that lasted longer than using Vr alone. Assimilating both Vr and Z has similar results as assimilating Vr alone, indicating dominant role of Vr data when analyzed using EnKF.

Ensemble forecasts starting from the EnKF analyses exhibit uncertainty growth in track, but not much growth in intensity spread. The latter is most likely due to the weakening of the hurricane itself during the forecast period. The experiment with 30-minute assimilation cycles shows similar results as the 10-minute cycles, while assimilating radar data at 60-minute intervals fails to obtain a strong enough vortex in both analysis and forecast. Additional experiments using single radars have also been conducted and will be reported elsewhere.

References:

Evensen, G., 1994: Sequential data assimilation with a nonlinear quasi-geostrophic model using Monte Carlo methods to forecast error statistics. J. Geophys. Res., 99 (C5), 10 143–10 162.

Houze, R. A., S. S. Chen, B. F. Smull, W.-C. Lee, and M. M. Bell, 2007: Hurricane intensity and eyewall replacement. Science, 315, 1235–1238.

Whitaker, J. S. and T. M. Hamill, 2002: Ensemble data assimilation without perturbed observations. M*on. Wea. Rev.,* 1**30,** 1913-1924.

Xue, M., K. K. Droegemeier, and V. Wong, 2000: The Advanced Regional Prediction System (ARPS) - A multiscale nonhydrostatic atmospheric simulation and prediction tool. Part I: Model dynamics and verification. Meteor. Atmos. Physics. 75, 161-193.

Xue, M., D.-H. Wang, J.-D. Gao, K. Brewster, and K. K. Droegemeier, 2003: The Advanced Regional Prediction System (ARPS), storm-scale numerical weather prediction and data assimilation. Meteor. Atmos. Physics, 82, 139-170.

Zhang, F., Y. Weng, J. A. Sippel, Z. Meng, and C. H. Bishop, 2009: Cloud-resolving Hurricane Initialization and Prediction through Assimilation of Doppler Radar Observations with an Ensemble Kalman Filter: Humberto (2007). *Monthl y Weather Review*, 137, 2105-2125.

Zhao, K. and M. Xue, 2009: Assimilation of coastal Doppler radar data with the ARPS 3DVAR and cloud analysis for the prediction of Hurricane Ike (2008). Geophy. Res. Letters, 36, L12803, doi:10.1029/2009GL038658.

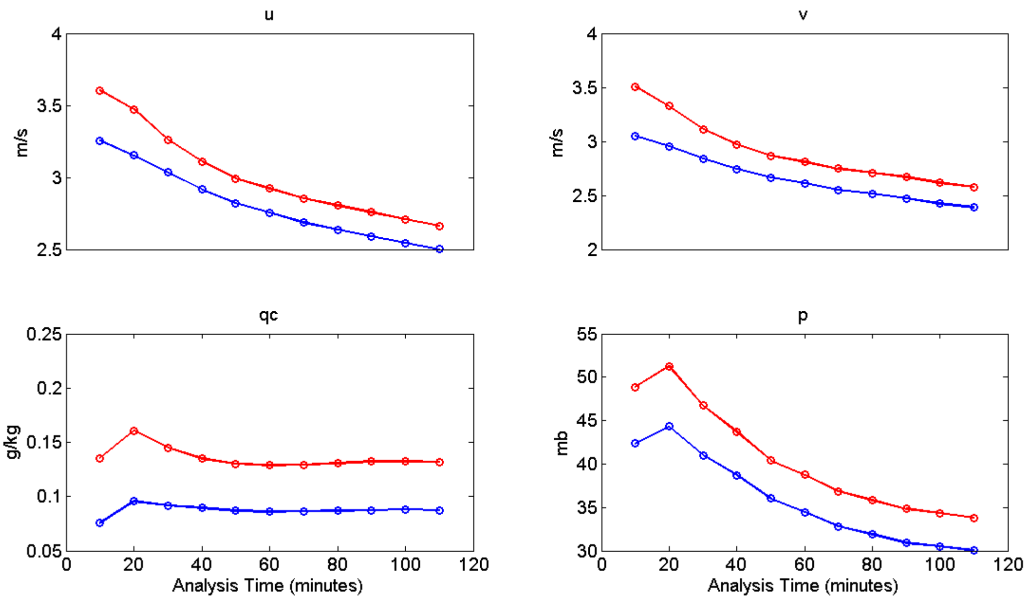

Fig. 1. Time evolution of ensemble forecast and analysis spread during the EnKF analysis cycles, spatially averaged in precipitation region (Z > 10 dBZ) for u, v, cloud water mixing ratio (q_c) and pressure, from experiment ExpAll. Those for the background forecast are in red and those for analysis are in blue.

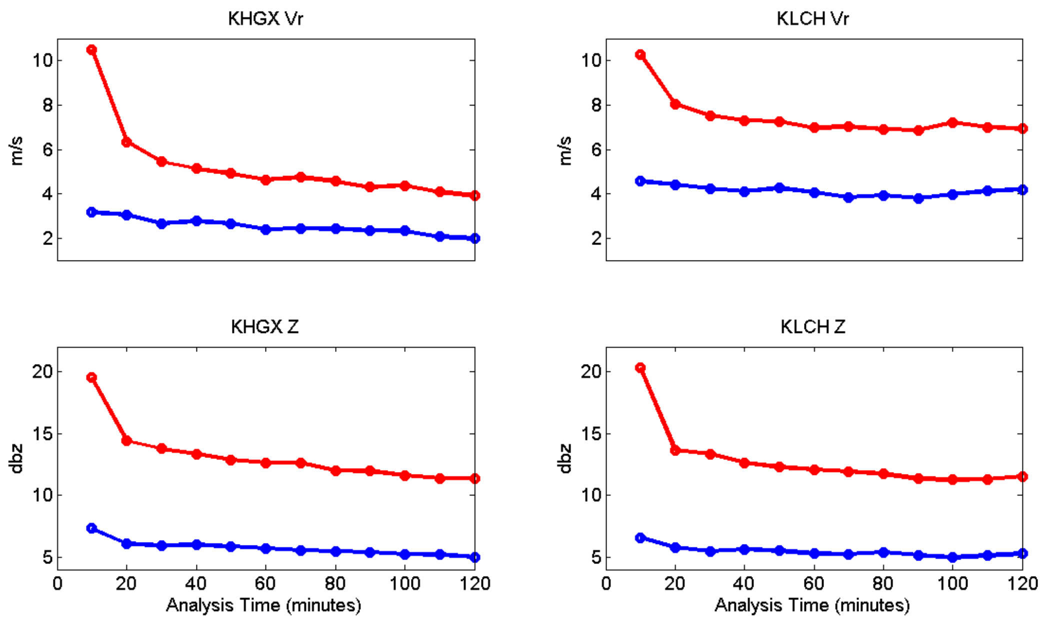

Fig. 2. Time evolution of innovation rms during the analysis cycles, averaged in precipitation region (Z > 10 dBZ) for Vr and Z of KHGX and KLCH, from experiment ExpAll. Those for the background forecast are in red and those for analysis are in blue.

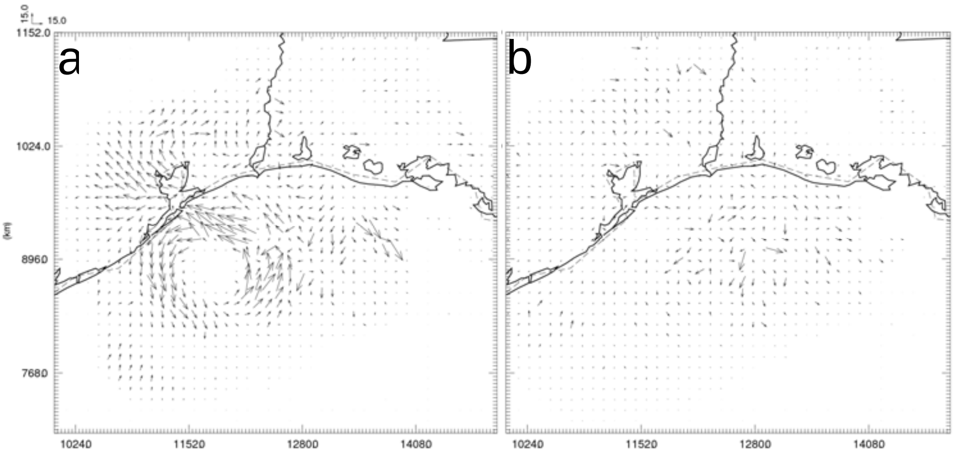

Fig. 3. Horizontal wind component increment at z=3km for (a) the first analysis and (b) the last analysis of ExpAll.

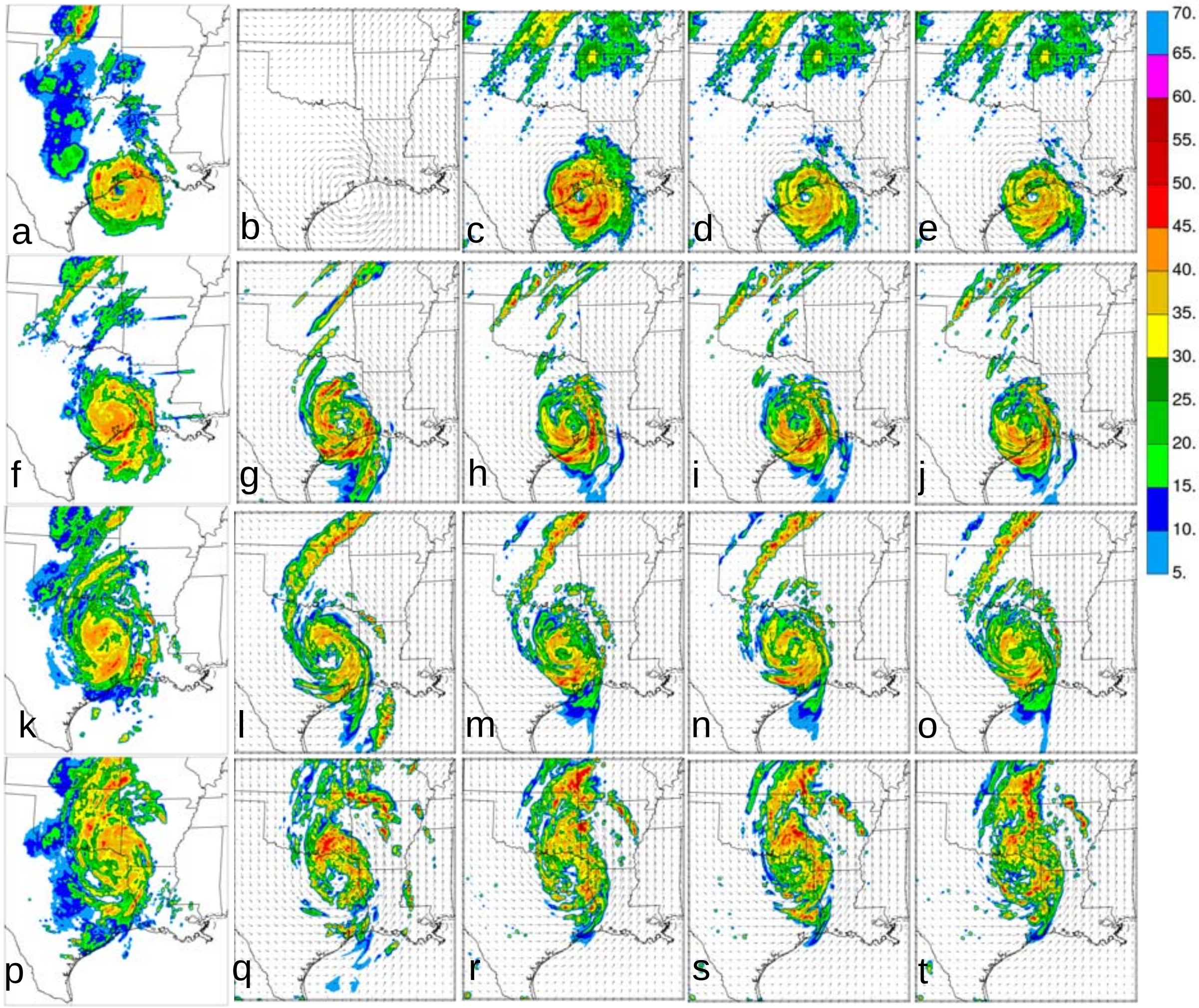

Fig. 4. Composite reflectivity (color shaded) and wind vectors at 3 km height analyzed and predicted by experiments (b, g, l and q) NoDA, (c, h, m and r) ExpZ, (d, i, n and s) ExpVr, and (e, j, o, t) ExpAll, as compared with (a, f, k and p) corresponding observations. The times shown are 0600, 1200, 1800 UTC, September 13 and 0000 UTC September 14, 2008.

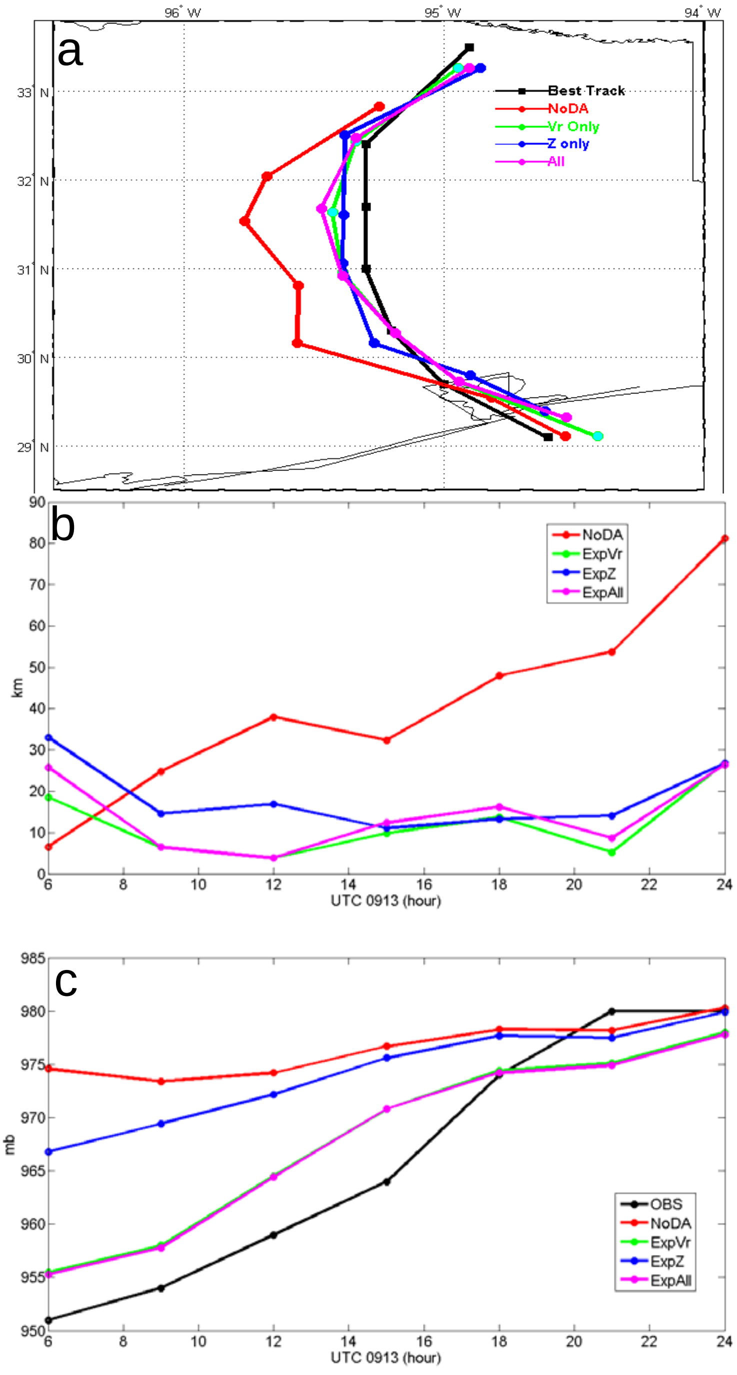

Fig. 5. The predicted (a) track, (b) intensity and (c) track error for Hurricane Ike, from 0600 UTC September 13 to 0000 UTC September 14.

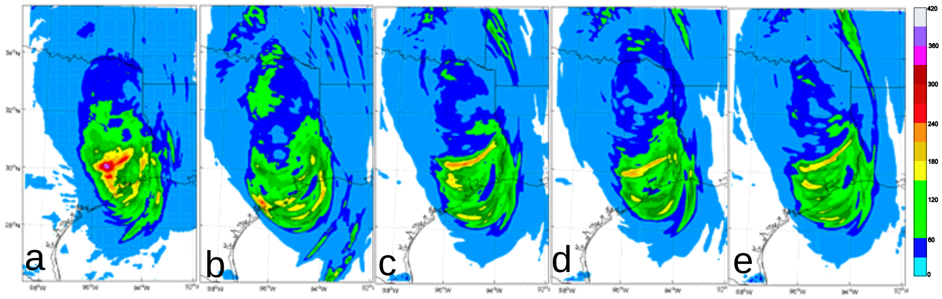

Fig. 6. 18-hour accumulated precipitation forecast from 0600 UTC September 13 to 0000 UTC September 14 for (a) observations, (b) NoDA, (c) ExpVr, (d) ExpZ and (e) ExpAll.

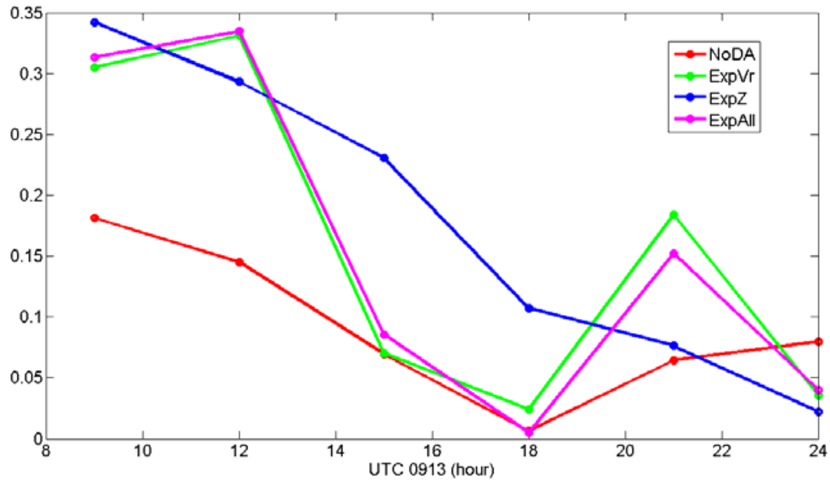

Fig. 7. ETS of 3-hour accumulated precipitation at the 30 mm threshold for NoDA, ExpVr, ExpZ and ExpAll.

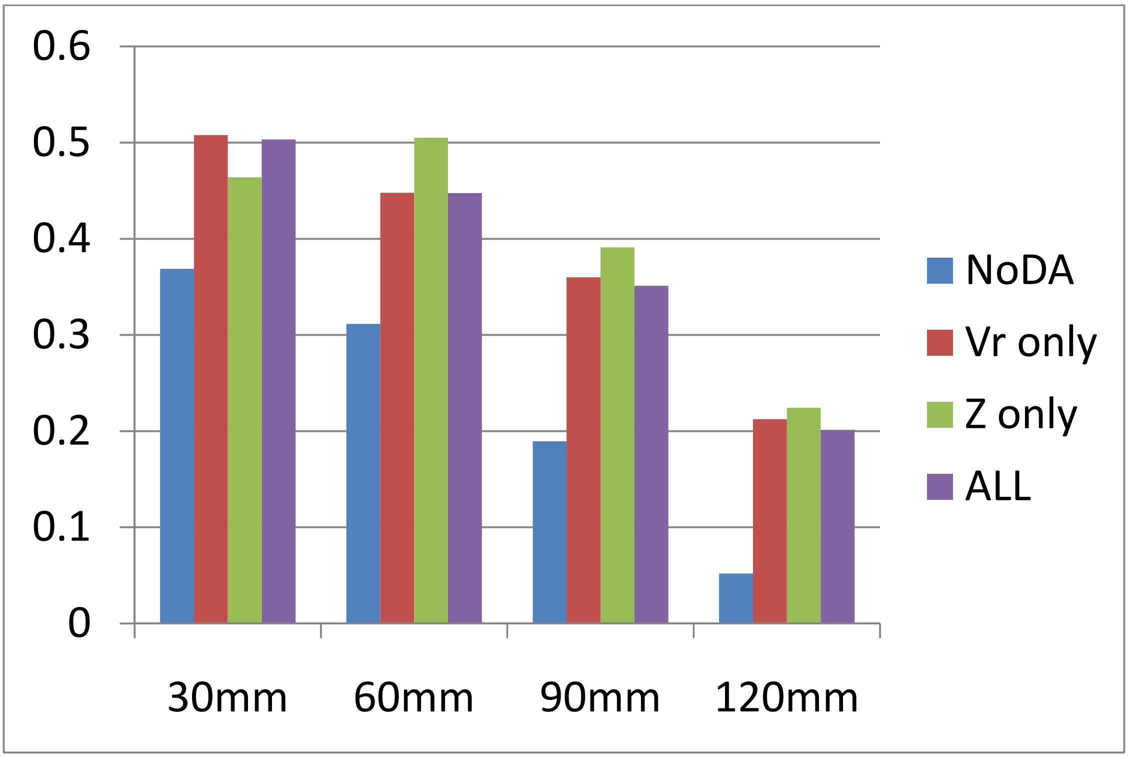

Fig. 8. ETS of 18-hour accumulated precipitation 0600 UTC September 13 to 0000 UTC September 14 at the threshold of 30 mm, 60 mm, 90 mm and 120 mm for NoDA, ExpVr, ExpZ and ExpAll.

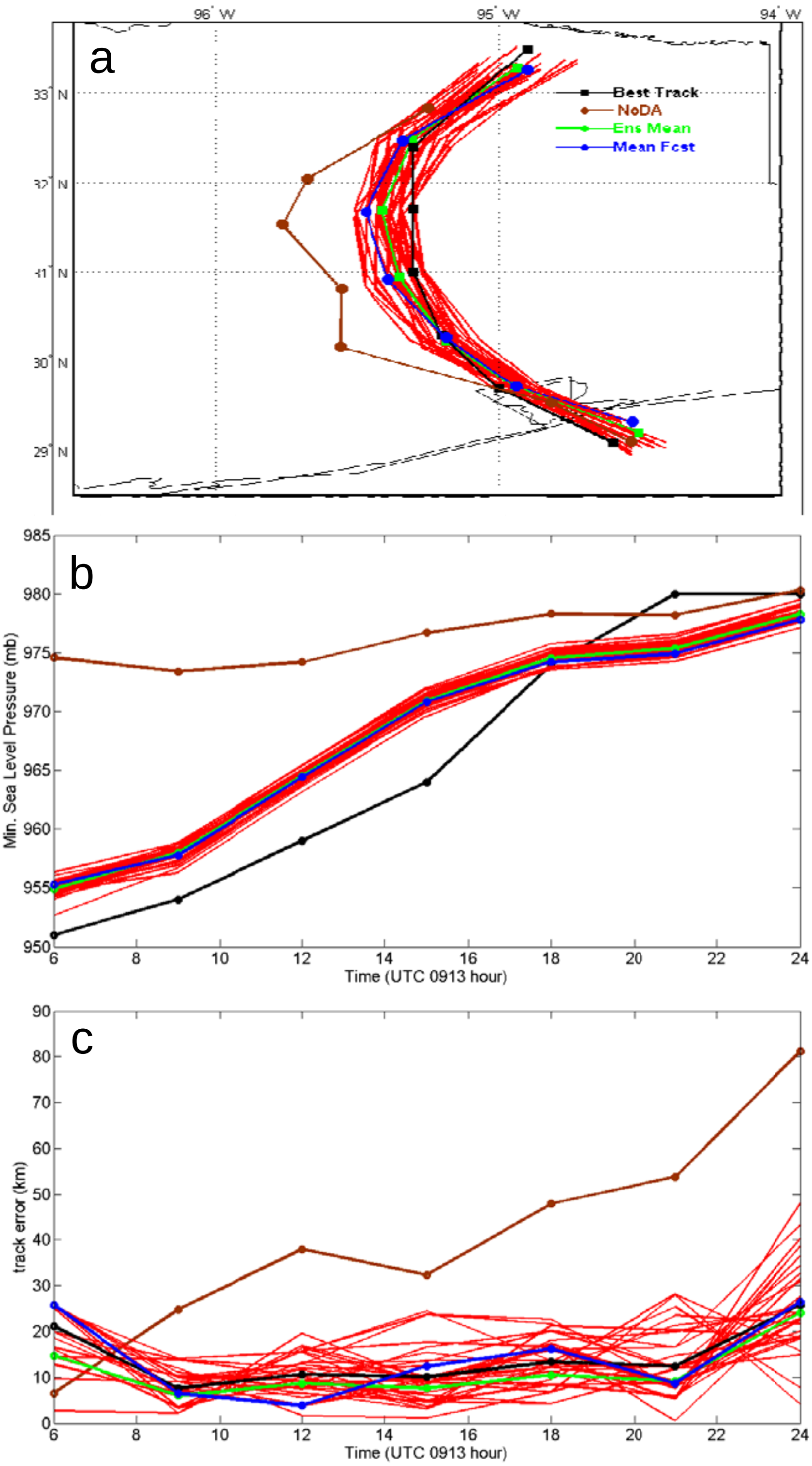

Fig. 9. The predicted ensemble (a) track, (b) minimum SLP and (c) track error for ExpAll (red), compared with the best track (black), NoDA (brown), ensemble average (green) and the deterministic forecast (blue).

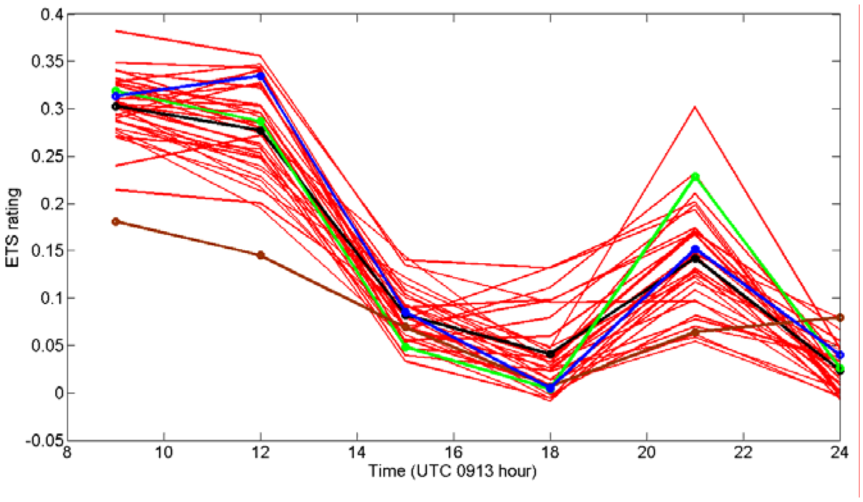

Fig. 10. The ensemble ETS of 3-hour accumulated precipitation for ExpAll (red), against NoDA (brown) and the deterministic forecast (blue).

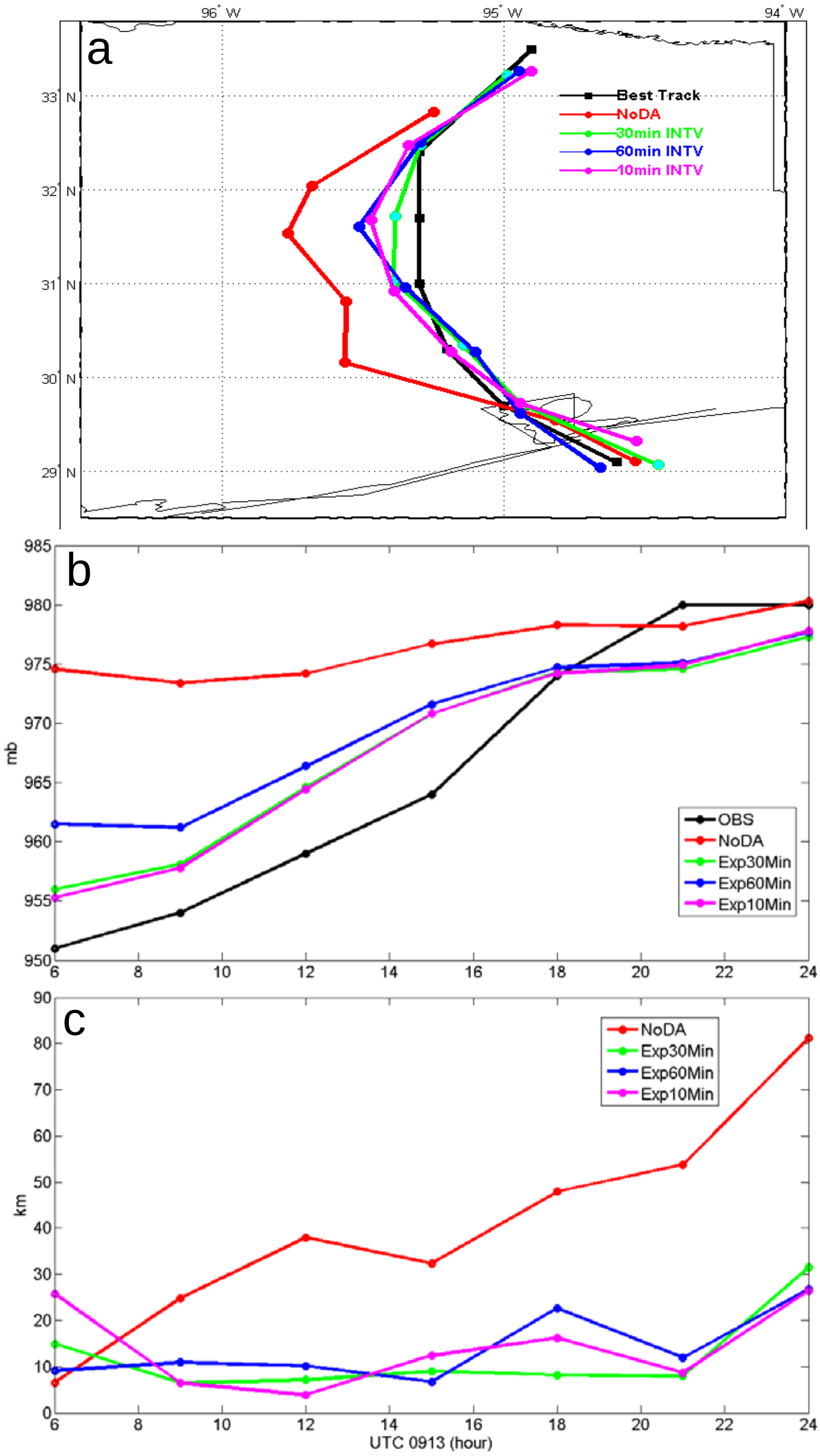

Fig. 11. The predicted (a) track, (b) minimum SLP and (c) track error for NoDA (red), Exp30Min (green), Exp60Min (blue) and ExpAll (also Exp10Min; magenta), compared with the best track (black).